Analysis of Morphological Variations in the Pubic Symphysis Using Three-Dimensional Statistical Shape Modeling

Yuyoung Kim

The Graduate School
Yonsei University
Department of Applied Life Science

Analysis of Morphological Variations in the Pubic Symphysis Using Three-Dimensional Statistical Shape Modeling

A Master's Thesis Submitted
to the Department of Applied Life Science
and the Graduate School of Yonsei University
in partial fulfillment of the
requirements for the degree of
Master of Science

Yuyoung Kim

December 2024

This certifies that the Master's Thesis of Yuyoung Kim is approved.

Kyung-Seok Hu

Thesis Supervisor Prof. Kyung-Seok Hu

Heejin Kim

Thesis Committee Member Prof. Hee-Jin Kim

Eun Jin Woo

Thesis Committee Member Prof. Eun Jin Woo

The Graduate School
Yonsei University
December 2024

TABLE OF CONTENTS

LIST OF FIGURES

LIST OF TABLES

ABSTRACT

Analysis of Morphological Variations in the Pubic Symphysis Using Three-Dimensional Statistical Shape Modeling

The pubic symphysis is pivotal in biological and forensic anthropology, particularly in age-at-death estimation. While computational approaches have advanced accuracy, they face limitations such as the "black box," obscuring crucial morphological features for estimation. Additionally, research on sexual dimorphism in the pubic symphysis is limited, often overlooking surface variations and relying on outline analyses.

To address these limitations, statistical shape modeling is employed, a method capable of analyzing complex morphological variations by generating mean models and identifying subtle shape changes. This research focuses on two primary aspects of pubic symphysis: sexual dimorphism and age-related morphological changes.

Computed Tomography scans of 252 subjects from the National Forensic Service of South Korea were analyzed. Preprocessed data underwent rigid alignment and statistical shape model construction. Principal component analysis was performed to compare models, followed by MATLAB-based classification training to assess variations.

Sexual dimorphism was most evident in dorsal-ventral width, influencing the outline shape beginning in the 30s and peaking in the 50s. In contrast, the 20s showed more significant differences in surface morphology rather than outline. Age-related changes were most pronounced in younger individuals, with males showing ventral margin extension and females experiencing changes likely linked to pregnancy. In older groups, changes were less significant and showed greater individual variability, particularly among females, due to menopause and pelvic muscle aging.

This study provides critical insights into the morphological complexity of the pubic symphysis. Thus, these findings can serve as valuable cornerstones for advancing human identification methodologies in biological and forensic anthropology.

Keywords: Pubic symphysis, Three-dimensional statistical shape modeling, Sexual dimorphism, Age-at-death estimation, Human variation, Forensic Anthropology

1. Introduction

Human identification, a fundamental objective in forensic anthropology, involves estimating biological characteristics or identifying unknown individuals to establish their identity (1-3). This process is essential for humanitarian purposes and serves as a foundation for addressing legal and judicial matters. Among the primary focus areas, the development of methods for estimating sex and age from skeletal remains has remained a central research topic.

Sex estimation primarily relies on analyzing measurements and morphological features, as male and female skeletons exhibit inherent differences in size and shape (1). Among various skeletal elements, the pelvic bone is considered the most sexually dimorphic, with regions such as the subpubic region, greater sciatic notch, and preauricular sulcus commonly utilized for this purpose (1,4-10). The cranium is another frequently analyzed skeletal element, with sex estimation often relying on five key morphological traits: the nuchal crest, mastoid process, supraorbital margin, glabella, and mental eminence (1,11-13).

In contrast to the relatively binary process of sex estimation, age estimation is inherently more complex. Various methods have been developed to estimate age, but environmental and cultural factors can influence skeletal changes in addition to natural skeletal aging processes (14-17). This complexity has led to ongoing debates about the applicability of age estimation methods across different populations (2). Nevertheless, widely employed approaches for adult age estimation include dental development and wear (18,19), cranial suture closure (1,20,21), and morphological changes in the pubic symphyseal surface (22-25). Additional skeletal features commonly analyzed for age estimation include the sternal rib end (26), clavicle (27), and iliac auricular surface (28).

Among skeletal elements, the pubic symphysis plays a central role in forensic anthropology due to its reliability in age estimation and inclusion in the highly sexually dimorphic pelvic bone (1,24,29). The pubic symphysis is predominantly utilized for estimating age, and several standardized methods have been developed to assess age based on phases or components (22,25,30,31). The Suchey-Brooks method, the most widely employed, classifies morphological changes in pubic symphysis into six phases characterized by features such as billowing, ossific nodules, and rim erosion (25,29,32). However, this method has notable limitations, including the subjective nature of visual assessments, significant overlaps in age ranges, and reduced accuracy in estimating older individuals' ages (33-35). Consequently, researchers often categorize unidentified individuals into broad age groups, such as young, middle-aged, or older adults, rather than providing precise age estimates.

To address these limitations, researchers have increasingly adopted mathematical approaches based on computed tomography to automate age estimation of the pubic symphysis. These approaches aim to provide more precise and quantitative results (36-42). Early computational methods focused on calculating convexity and concavity, noting that the symphyseal surface becomes flatter with age (36,37). Subsequent analyses utilized bending energy calculations through thin plate splines (TPS) algorithm or variance-based SAH scores proposed by Slice and Algee-Hewitt to assess surface morphology (38-41). Despite advancements, many methods struggled to accurately estimate older individuals' ages due to underrepresented subtle morphological variations (39-41). Recently, Kotěrová et al. introduced algorithms such as the Simple Automated Symphyseal Surface-based (SASS) and the Advanced Automated Neural Network-grounded Extended Symphyseal Surface-based (AANNESS), which demonstrated improved accuracy by analyzing subtle morphological changes across diverse populations and sexes (42).

While computational approaches have enhanced age estimation, they often focus on subtle morphological differences without addressing the broader, fundamental changes occurring in the pubic symphysis over time. Moreover, these methods frequently operate as a "black box," failing to elucidate the specific features used for classification. Castillo et al. sought to address this issue by examining morphological changes in the pubic symphysis across various age groups (43). However, their study lacked detailed insights into the direction or magnitude of these changes, limiting its applicability.

Furthermore, while sexual dimorphism is a critical factor in pubic symphyseal morphology, it remains underexplored in computational studies. Although numerous studies have examined sexual dimorphism in the pelvic bone (4-9), few have explicitly focused on the pubic symphysis (22,24,44). Seminal works, including those by Todd and Suchey-Brooks, acknowledged sex-specific variations in the pubic symphysis and recommended sex-specific approaches to age estimation (22,25). However, these studies often lacked quantitative analyses of sexual dimorphic traits.

Recently, Bravo Morante et al. used geometric morphometric methods to analyze sexual dimorphism in the pubic symphysis, focusing primarily on the outline (44). While this study provided valuable insights, its reliance on a few landmarks likely overlooked finer morphological details. Additionally, potential surface morphology differences on the symphyseal surface were not fully explored and may have been disregarded. In contrast, Lottering et al. rendered the symphyseal surface in three dimensions, which provided a more detailed representation of its morphology. They demonstrated that males exhibited larger surface dimensions than females. However, their findings were categorized according to the Suchey-Brooks phases, limiting their ability to delineate sexual dimorphism across specific age groups. Moreover, the extent of sexual dimorphism was not quantitatively assessed, further underscoring the need for a comprehensive analytical framework (45).

These limitations highlight the need for a more comprehensive approach to understanding sexual dimorphism and age-related changes in the pubic symphysis. A detailed examination that captures both outline and surface-level variations while quantitatively characterizing sexual dimorphism across age groups is essential for advancing forensic anthropology methodologies.

To fill these gaps, this study employs statistical shape modeling (SSM) to examine sexual dimorphism and age-related morphological changes in the pubic symphysis. It specifically seeks to overcome gaps in previous research, including the limited focus on subtle morphological variations, insufficient insights into the direction and magnitude of age-related changes, lack of quantitative analyses of sexual dimorphism, and reliance on phase-based categorizations. this study aims to achieve the following objectives: visualizing morphological differences and changes in the pubic symphysis associated with sexual dimorphism and aging, estimating structural and biomechanical factors underlying these changes, and identifying key morphological variations for distinguishing between sexes and consecutive age groups. The findings are anticipated to enhance forensic anthropology by improving the precision of sex and age estimation methodologies and providing critical tools for human identification. Furthermore, by leveraging SSM, this research introduces a novel quantitative framework for evaluating subtle morphological changes, offering valuable implications for both academic and practical advancements in forensic science.

2. Materials and methods

2.1. Materials

A total of 641 CT scans of adults whose bodies underwent forensic examination by South Korea's National Forensic Service between 2020 and 2021 were obtained for the study. This study included South Korean nationals for whom premortem details like sex and age were available. Following careful review, individuals with pubis bones displaying pathology or damage were excluded. For each age decade from the twenties to the eighties, 18 males and 18 females were randomly chosen for analysis, resulting in a total of 252 individuals. A detailed age distribution is presented in Table 1. Approval of the use of CT data (protocol number 2-2023-0071) was obtained from the Institutional Review Board of Yonsei University, College of Dentistry in Seoul, which waived the requirement for informed consent from all subjects and/or their legal guardians. All methods were performed in accordance with the relevant guidelines and regulations.

Table 1. Age distribution of subjects by decade.

Age groups	Mean age ± Standard deviation		
	Male	**Female**	**Total**
20s	23.8 ± 2.6	23.9 ± 2.9	23.9 ± 2.7
30s	34.8 ± 2.6	34.2 ± 3.0	34.5 ± 2.8
40s	45.4 ± 3.0	45.4 ± 2.8	45.4 ± 2.9
50s	53.8 ± 2.5	55.1 ± 2.7	54.5 ± 2.7
60s	63.2 ± 2.5	63.4 ± 2.4	63.3 ± 2.4
70s	73.8 ± 2.5	73.9 ± 2.6	73.9 ± 2.5
80s	82.8 ± 2.6	84.7 ± 3.2	83.8 ± 3.0

2.2. Data acquisition

Whole-body CT data were stored in Digital Imaging and Communication in Medicine (DICOM) format. To isolate the pubic symphysis for analysis, 3D Slicer (version 5.3.0) and Meshmixer (version 3.5.474) were employed.

The data acquisition involved three key steps. First, CT data was imported into 3D Slicer, where the *Volume Rendering* and *Crop Volume* modules were used to locate the pubic symphysis and set a region of interest (ROI) to isolate it. Next, the *Threshold* Effect of the *Segmentation Editor module* was applied within the ROI to remove surrounding soft tissues and create a complete model of the pubic symphysis, with threshold values adjusted to each subject's bone density. Finally, in Meshmixer, the left and right pubic bones were separated to examine the pubic symphysis, and any remaining soft tissues were removed. For this study, only the left pubic symphysis was used for analysis under the assumption of bilateral asymmetry in the human skeleton (46). The processed data was then saved in Polygon File (PLY) format.

2.3. Preprocessing

The segmented data frequently contains substantial noise and extraneous mesh elements unrelated to anatomical structures, necessitating a preprocessing step to eliminate these artifacts and refine the data for shape analysis and modeling. This preprocessing, commonly called "mesh cleaning," was conducted using MeshLab (version 2022.02) and Meshmixer.

The overall process comprised three main stages, as outlined in Figure 1. In the first stage, elements that could interfere with shape analysis were removed using MeshLab's tools, such as the *select faces in rectangular region*, *fit plane to selection*, *ambient occlusion*, *select faces by color*, and *delete selected face and vertices* filters (Figure 1A). These filters left only the outer shell of the pubic symphysis data intact. In the second stage, hollow regions were made watertight using the *make solid* function in Meshmixer, eliminating any internal elements that could influence the analysis (Figure 1B). Finally, the pubic symphysis data were smoothed in MeshLab using the *screened Poisson surface reconstruction*, *isotropic explicit remeshing*, and *remove duplicate vertex and faces* filters (Figure 1C). This final stage smoothed the surface and redistributed vertices, producing a consistent data topology suited for subsequent analysis.

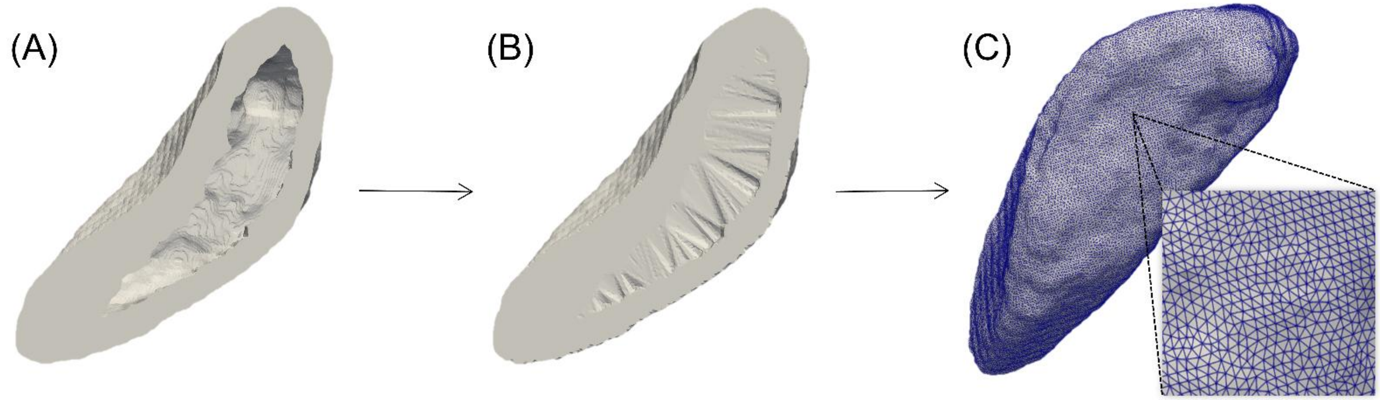

Figure 1. Three-step preprocessing procedure.

Mesh cleaning removes extraneous bone mesh elements (A, B) and redistributes vertex data for topology refinement (C).

2.4. Statistical shape modeling

2.4.1. Concept and Application

Shape refers to the geometric information that remains after excluding global geometric properties – translation, orientation, and size (47,48). Starting from D'Arcy Thompson, shape analysis has become a fundamental tool for quantitative morphology analysis (49). Among its methods, statistical shape modeling (SSM) is imperative in analyzing and understanding the range of morphological variations within a defined shape group (50,51). Its ability to generate mean models and depict shape variation across populations makes it ideal for studying complex and variable structures. As a result, SSM has been applied in biological sciences, including assessing anatomical variations (52-54), developing segmentation methods for computed tomography (CT) and magnetic resonance imaging (MRI) (50,55,56), and evaluating pathological changes in morphology (57,58).

Until recently, SSM has played a minor role in biological anthropology. However, its application in this field has expanded notably in recent years.

Audenaert et al. utilized SSM to analyze sexual dimorphism across seven lower limb anatomical structures from CT scans of 271 individuals, identifying size as the most significant factor for sex discrimination with only slight improvements over traditional methods (51). Likewise, Fliss et al. analyzed 61 femur CT scans to estimate sex using SSM, finding that classification accuracy improved by including more principal components. However, accuracy itself was similar to traditional linear measurements (59).

SSM has also been utilized to analyze age-related morphological changes. Shin et al. constructed a shape model of axial cervical vertebrae from 43 individuals to assess skeletal maturation, finding that skeletal maturation in males could be predicted more accurately than in females. Additionally, they observed no significant correlation between bone size and skeletal maturity (60). Similarly, Klop et al. created shape models from 874 cadaveric children's mandibles to analyze growing morphology, visualizing the most important shape variation correlated with age (61).

SSM has also been applied to estimate stature. Ebert et al. reconstructed 42 left femora into their original forms using SSM, achieving minimal reconstruction errors that enabled reliable stature estimations. Additionally, sex estimation based on constructed models demonstrated relatively high accuracy, with rates reaching approximately 85% for single-sided cut (62).

Previous studies employing SSM in biological anthropology have primarily focused on identifying significant shape variations related to sex or age, thereby improving the accuracy of human identification. Applying SSM to the pubic symphysis is expected to reveal meaningful morphological variations that differentiate sex or age groups. Moreover, although not a primary focus, previous research has used SSM to generate mean models for specific groups (e.g., by sex), uncovering morphological traits that are difficult to detect visually. Given the complex and variable morphology of the pubic symphysis, the methodological advantages of SSM make it particularly well-suited for its analysis.

This study used open-source software ShapeWorks (version 6.3.2) to construct statistical shape models. ShapeWorks was selected for its full graphical user interface, which eliminates the need for coding in environments such as MATLAB or R. Additionally, it provides the convenience of handling preprocessing and analysis within a single software. Another reason for choosing ShapeWorks is its use of Particle-based Surface Modeling (PSM), a method known for constructing precise and robust statistical shape models (further discussed in Section 2.4.3) (63).

The SSM process comprises three main steps: mesh optimization, shape registration, and principal component analysis (PCA). Below are detailed explanations of each step.

2.4.2. Initial alignment and ROI

The initial alignment process aimed to convert the pubic symphysis data into a format compatible with ShapeWorks (Figure 2). All steps were performed within ShapeWorks' *data* and *grooming* module.

For shape analysis, it was necessary to align shapes oriented in different positions and directions to ensure that only intrinsic shape variations were captured, independent of positional differences. Therefore, an initial alignment was required to arrange the data for consistent orientation. Five anatomical landmarks were manually designated on the sample data to achieve consistent alignment, and the Iterative Closest Point (ICP) algorithm was then applied to align these landmarks across 252 pubic symphysis samples (63). These landmarks included the midpoint of the dorsal (DM) and ventral (VM) margins, the superior (SP) and inferior (IP) points of the symphyseal surface, and a central point (CP) at the intersection of lines connecting DM to VM and SP to IP (Figure 2A). Based on these five landmarks, thousands of vertices on each of the 252 pubic symphysis samples were aligned.

Additionally, previous studies on pubic symphysis morphology have indicated that morphological differences or changes associated with sex or age extend beyond the symphyseal surface (64). This included areas surrounding the articulation margins. Therefore, by following the protocol established by Kotěrová et al., This study limits the analysis to a 1 cm region extending vertically from each articulation margin (42), ensuring that areas beyond this region are not included (Figure 2B).

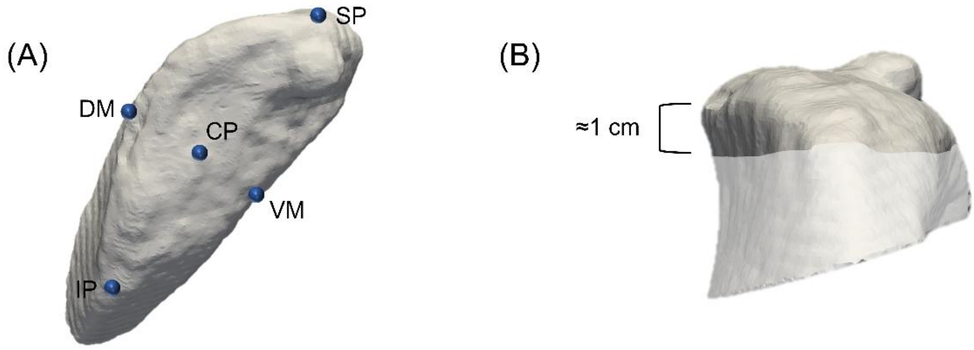

Figure 2. Initial alignment and ROI designation.

The mesh optimization procedure prepares the pubic symphysis data for use in ShapeWorks. For consistent alignment, five key anatomical landmarks were manually identified (A): the superior (SP), inferior (IP), ventral (VM), dorsal (DM), and central points of the symphyseal surface (CP). Following this, the region of interest (ROI) was narrowed to a 1 cm vertical span from each articulation margin, concentrating the analysis on this area (B).

2.4.3. Shape model construction

To construct SSM, the vertices of each dataset should correspond to each other, and the corresponding vertices should represent a similar position or feature in each dataset. ShapeWorks employs a PSM algorithm to ensure correspondence among vertices. PSM positions landmarks based on entropy, strategically concentrating them in areas of greater shape variability (47,63). In this study, 4096 landmarks were automatically designated on rigidly aligned data using PSM.

Furthermore, Procrustes registration was performed to achieve a more accurate and consistent alignment of shapes for subsequent statistical analysis (65). This involved scaling, translation, and rotation of the shapes to minimize the differences between corresponding points while preserving their distinct morphological features.

2.5. Shape model analysis

2.5.1. Principal component analysis

Principal component analysis (PCA) was employed to capture shape variation within the dataset. PCA is a statistical technique that reduces the dimensionality of high-dimensional shape data while preserving essential information. By decomposing the covariance matrix of the aligned shape data into eigenvectors and eigenvalues, PCA facilitated the identification of principal components (PCs) that explain the majority of variance in the dataset (66). These PCs represent distinct shape variations, offering valuable insights into the dataset's underlying dynamics of shape variation.

During PCA, the mean model of each sex or age group is extracted, portraying the average shape within the respective group. The mean model later serves as a reference for comparing between sexes or age groups, offering quantitative and visual descriptions of sexual dimorphism or age-related morphological changes.

2.5.2. Model evaluation

Three commonly used metrics—compactness, generalization, and specificity—were employed to evaluate the statistical shape model quantitatively (47,67). These metrics ensure the model creates an optimal representation of shape variation while balancing simplicity and accuracy (67). Since the same dataset was used in this study to investigate sexual dimorphism and aging morphology, the model evaluation results apply to both analyses.

Compactness indicates the efficiency of the shape model, assessing whether a wide range of morphological variations could be reproduced with a small number of PCs.

Generalization evaluates the ability of the generated PC model to reconstruct shapes beyond the dataset used for analysis. This is assessed by the error value between unseen data and reconstructed data. Lastly, specificity evaluates the capacity of the PC model to produce reasonable shape data randomly. It is considered ideal when the error value between the random shape data and the closest sample data minimally increases as the number of PCs used increases.

2.5.3. Model comparison

Using the *model-to-model distance* module of SlicerSALT (version 4.0.1), the spatial displacement of corresponding landmarks was visualized with vector arrows and heatmaps. The morphological differences between males and females were demonstrated in the first part of the study. For the second part of the study, the morphological changes from the younger age group to the older age group were illustrated (e.g., the morphological characteristic of the average pubic symphysis of individuals in their 30s compared to those in their 20s).

To evaluate the statistical significance of observed morphological changes, Hotelling's T-squared test was applied ($p<0.05$) (63). Regions with p-values exceeding 0.05, indicating non-significant differences, were colored blue. In contrast, areas with p-values below 0.05 were displayed in a gradient based on significance levels, with the most significant regions highlighted in red.

2.5.4. Shape-based classification

The accuracy of group classification based on morphological characteristics was evaluated using the Classification Learner application in MATLAB (version R2023a). In the analysis of sexual dimorphism, sex was set as the response variable, with each sample's PCA scores of the compared two groups used as predictor variables. For the analysis of age-related morphological variations, age group served as the response variable, while PCA scores were again used as predictors. All available training algorithms in MATLAB were utilized, with training conducted through 10-fold cross-validation. For each comparison, the algorithm achieving the highest classification accuracy was selected, and the principal component (PC) most influential in distinguishing consecutive age groups was identified via an ANOVA-based feature ranking method.

3. Results

3.1. Model evaluation

Figure 3 presents the three quantitative evaluations of the constructed statistical shape model based on 252 datasets.

Compactness (Figure 1A) demonstrates the efficiency of capturing morphological variation. Results indicate that the top ten principal components (PCs) account for about 85% of the shape variability in the pubic symphysis data, while the top 20 PCs capture approximately 95%.

Generalization (Figure 1B) assesses the PCA model's ability to reconstruct shapes beyond the dataset used in the analysis, measured by the error between the original and reconstructed data. Results show that increasing the number of PCs reduced the error value from roughly 0.6 mm to 0.2 mm.

Finally, specificity (Figure 1C) measures whether the PCA model can randomly generate realistic shape models based on the error between the random model and its nearest sample model. While more PCs add complexity, this increase should be gradual. In this study, specificity results showed a minimal increase in error values up to around 0.2 mm when up to 20 PCs were used.

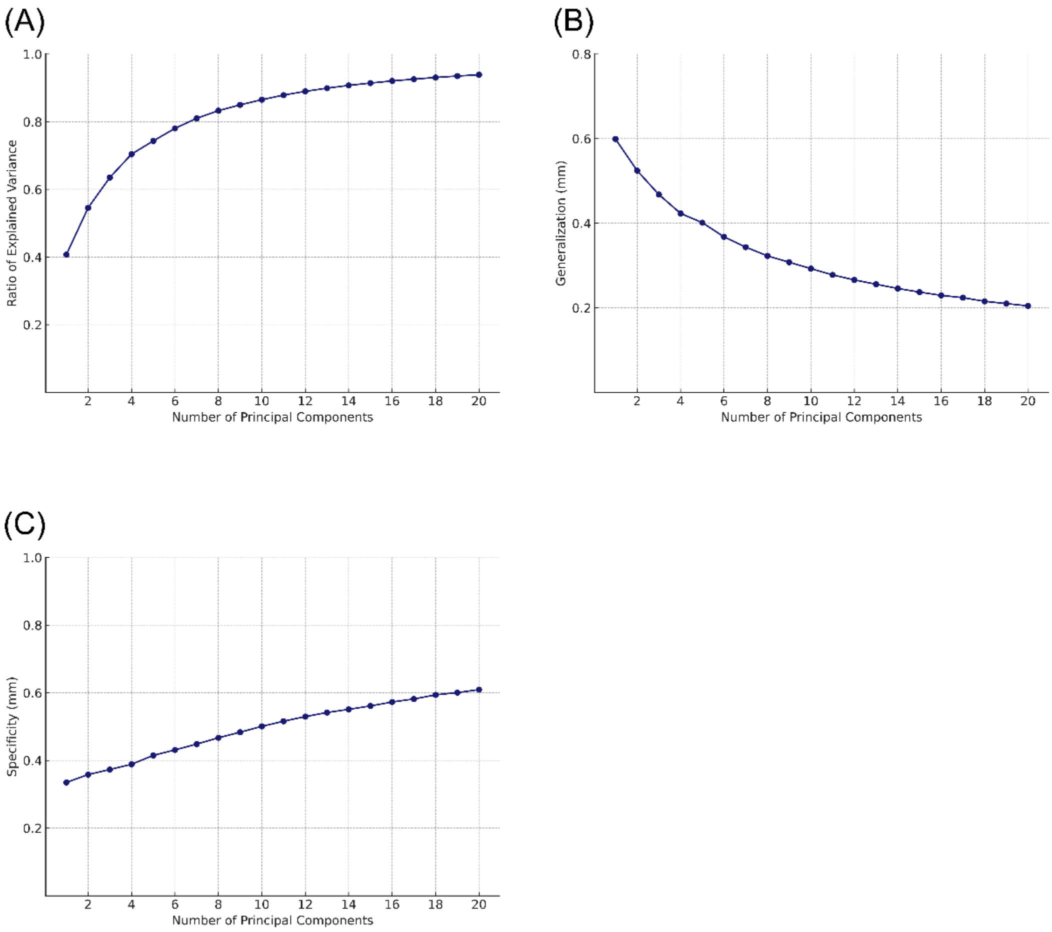

Figure 3. Graphs for shape model evaluation.

Compactness (A) illustrates whether the PC model can capture a wide range of shape variations using a limited number of PCs. Generalization (B) assesses the model's ability to reconstruct shapes not included in the sample data, measured by the error between unseen and reconstructed data. Specificity (C) evaluates the model's capacity to randomly generate realistic shape data based on the error between the randomly generated data and the closest sample data.

3.2. Principal Components

Figure 4 demonstrates the first five principal components (PCs) obtained from the PCA of 252 pubic symphyseal surface datasets.

Each PC captures unique morphological characteristics: PC1 represents the overall width of the symphyseal surface; PC2 indicates whether the central margin extends ventrally or dorsally; PC3 emphasizes the combination of the sharpness at the inferior point and the curvature of the ventral or dorsal margin; PC4 highlights the degree of bulging in either the central or marginal areas of the symphyseal surface; and PC5 focuses on the prominence of the superior, central, or inferior third of the surface.

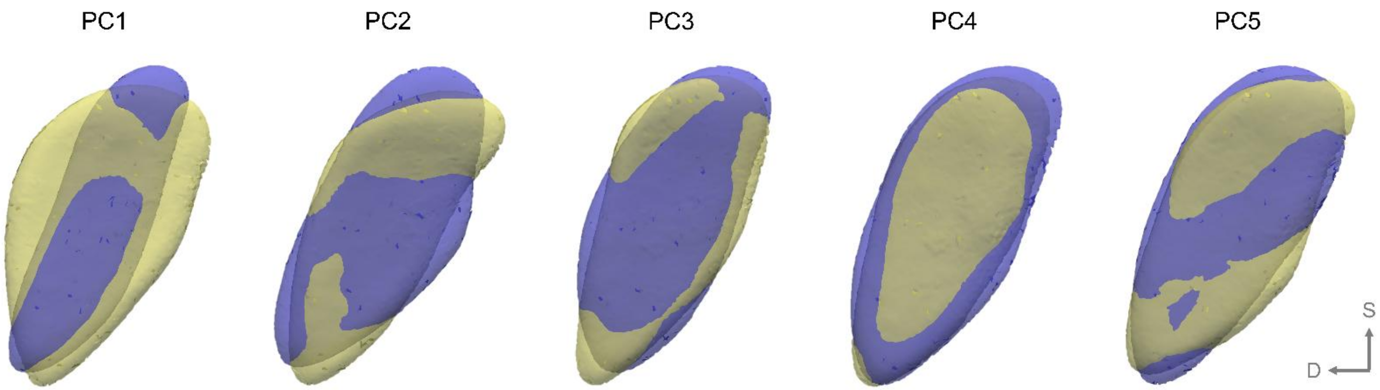

Figure 4. Shape variations of PC 1 through PC 5.

A model with a weight of -2 standard deviations (in violet) is overlaid with a model of +2 standard deviations (in yellow). Areas where the two models overlap are displayed in colors other than violet or yellow. Each principal component (PC) represents one or more unique morphological variations. In the orientation labels, 'D' stands for dorsal, and 'S' stands for superior.

3.3. Mean models

Mean pubic symphysis models were constructed for each sex and each age-sex group. The detailed description is as follows.

First, for sex-specific mean models (Figure 5), males exhibited a wider symphyseal surface in the dorsal-ventral direction than females. Additionally, the inferior point in males appeared sharper than in females. In both sexes, the dorsal border of the symphyseal surface was rounded, whereas the ventral border was straighter, forming a subtle angle at the midpoint.

Next, for age-sex group mean models (Figure 6), the mean model for individuals in their twenties demonstrated distinct morphological characteristics compared to other age groups. Specifically, the symphyseal surface in this group was predominantly oval-shaped, with rounded superior and inferior points. In contrast, the inferior points in other age groups tended to be more tapered. From the thirties to the eighties, the mean models displayed a flatter or slightly recessed symphyseal surface, whereas the twenties group retained a degree of convexity. Furthermore, the width of the symphyseal surface increased with age in males, while in females, the width remained relatively consistent across age groups.

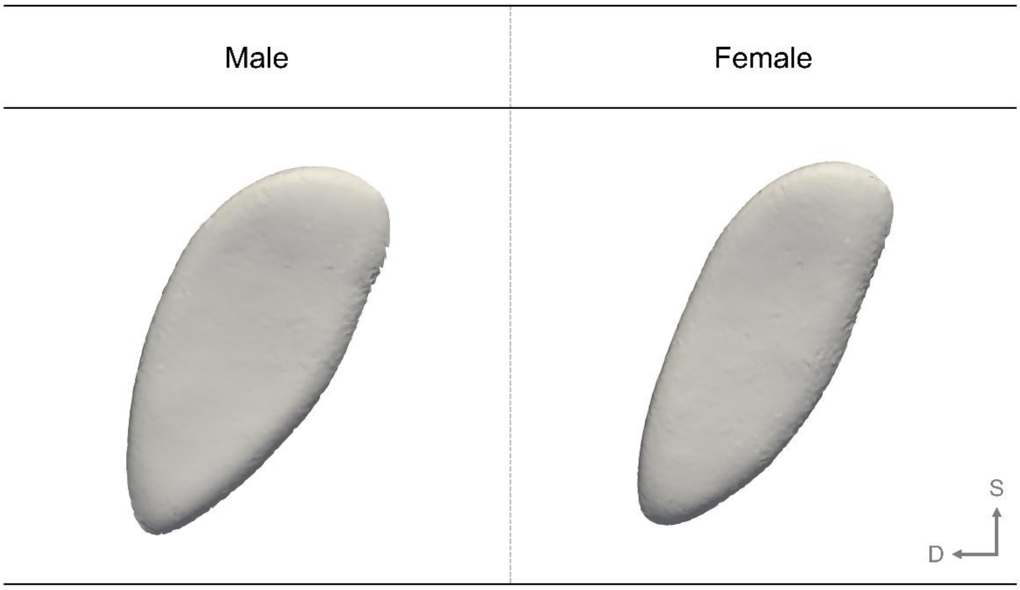

Figure 5. Mean models of the pubic symphysis of male and female.
For orientation labels, ‘D’ represents dorsal, and ‘S’ represents superior.

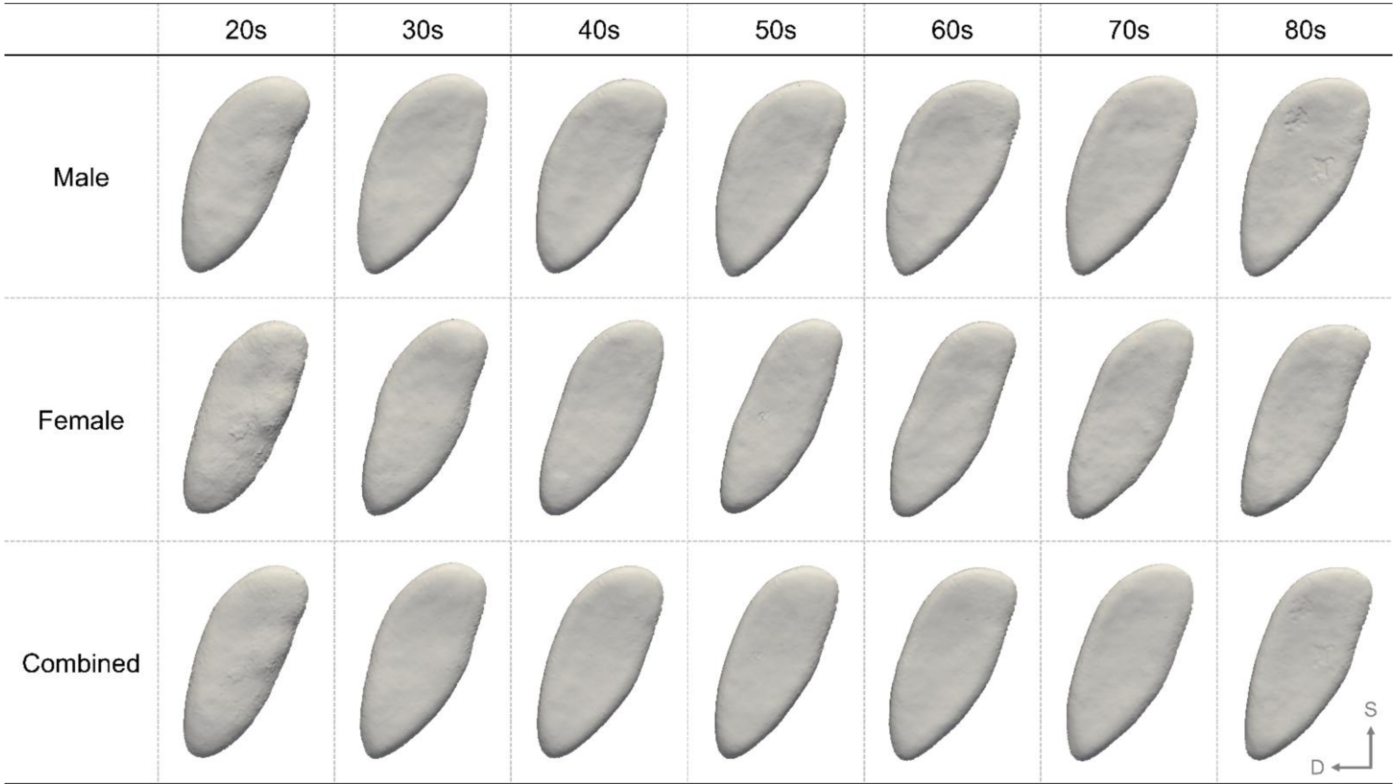

Figure 6. Mean models of the pubic symphysis by sex and age group.
For orientation labels, ‘D’ represents dorsal, and ‘S’ represents superior.

3.4. Sexual dimorphism

3.4.1. Model comparison

The morphological differences between the mean female and male pubic symphyses were analyzed and demonstrated, accompanied by statistical testing of these differences (Figure 7). Additionally, sexually dimorphic features in the mean pubic symphysis models for each age group were visualized and the statistical significance of these changes was evaluated (Figure 8).

When comparing the mean surfaces irrespective of age (Figure 7), females exhibited narrower dorsal-ventral widths than males. Additionally, the superior point of the female surface appeared to extend further superiorly, while the inferior angle was inclined dorsally. Among these sexually dimorphic features, the difference in dorsal-ventral width was the most significant. Statistical testing revealed that nearly all surface differences between sexes were statistically significant, except for a small region in the center of the surface.

The sexual dimorphism observed in each age group is described as follows (Figure 8).

Sexual dimorphism in surface morphology was most pronounced in females in their twenties. Females exhibited a more dorsal positioning of the superior and inferior angles and the surrounding surfaces. Additionally, the middle section of the ventral border and the adjacent surfaces appeared more ventrally prominent in females.

From the thirties to the eighties, morphological differences between males and females began to follow a distinct pattern, particularly in the outline of the surface. Females typically displayed a narrower surface, a superior angle extending further upward, and an inferior angle inclined dorsally. Notably, these morphological differences gradually increased with age, reaching their peak in the fifties. However, after the fifties, the degree of sexual dimorphism began to diminish.

The results of the statistical testing for morphological differences across age groups showed a pattern consistent with the shape comparison (Figure 8). The statistically significant morphological differences increased and extended across the surface up to the 50s, marking the peak of sexual dimorphism. Beyond the 50s, the extent of statistically significant areas began to decrease with age.

In the 20s, significant areas were primarily confined to the center of the surface and regions near the superior and inferior angles. However, from the 30s to the 80s, significant areas became more concentrated along the ventral and dorsal borders and the adjacent surfaces, excluding the central portion of the surface.

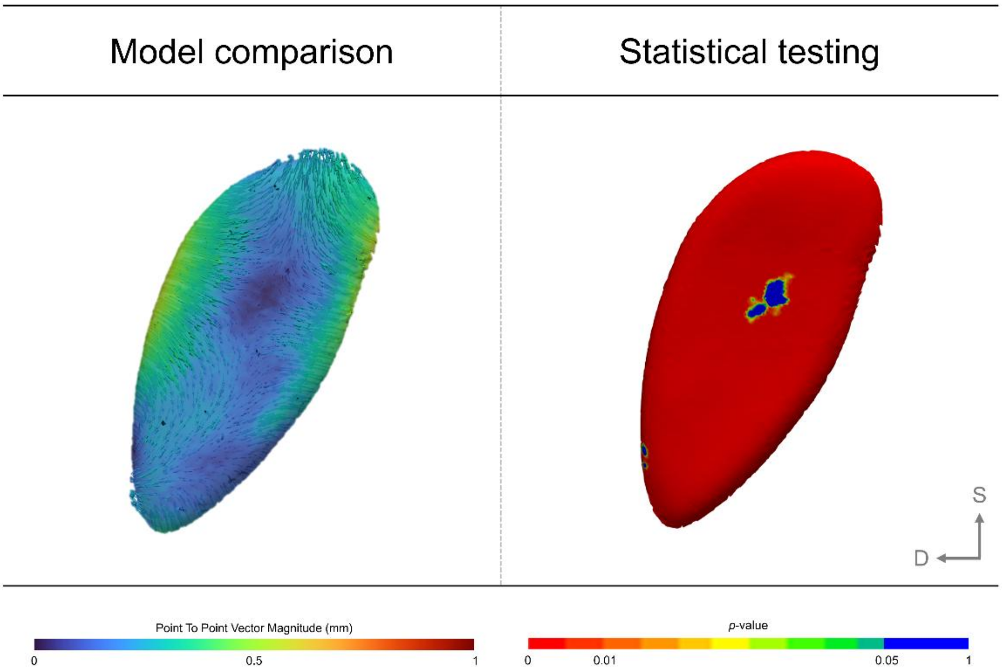

Figure 7. Sexual dimorphism in the pubic symphysis.

(Left) Three-dimensional visualization of the relative differences that the female pubic symphysis exhibits to that of the male, with vector arrows indicating the direction and magnitude of changes, doubled in size for clarity.

(Right) Regions with p-values above 0.05 are shown in blue, while those below 0.05 are color-coded by significance level, with the most significant changes marked in red.

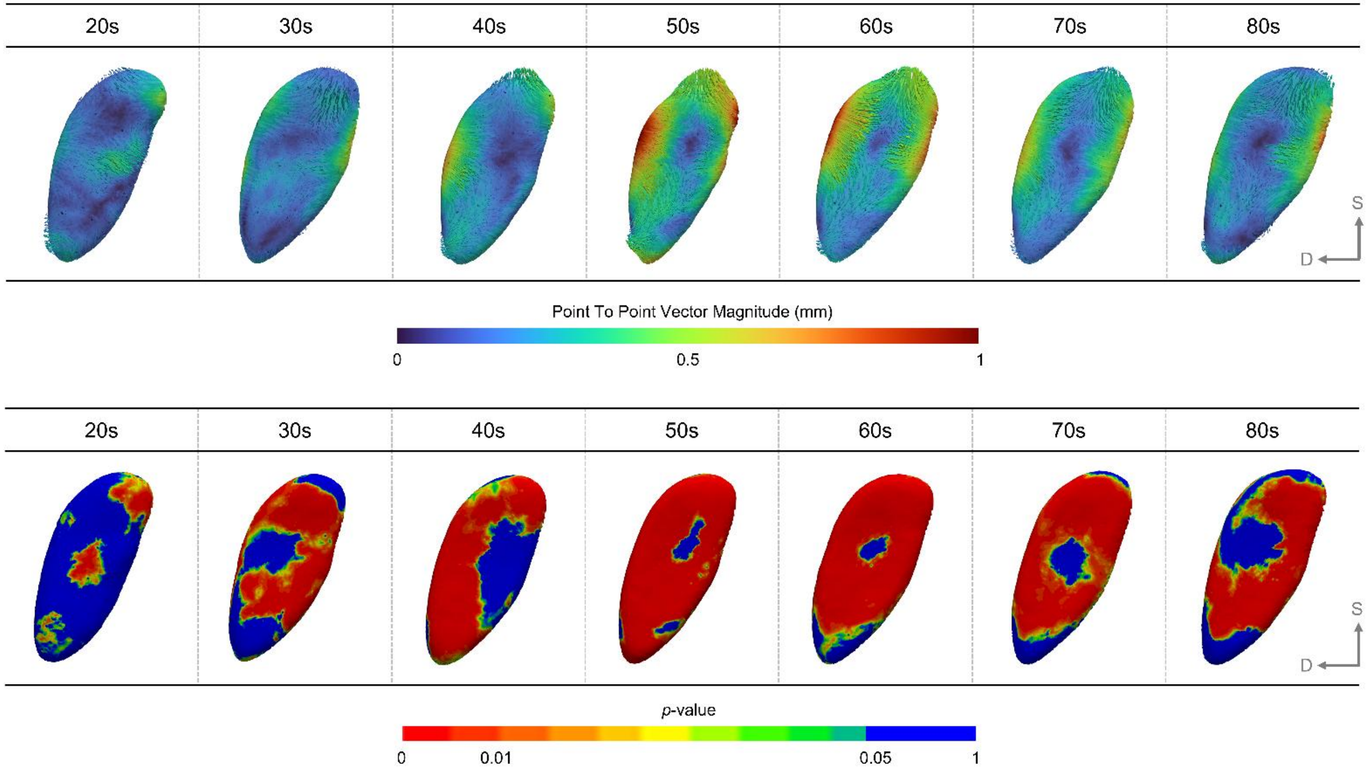

Figure 8. Sexual dimorphism in each age group.

Model comparison (top line) and statistical testing of morphological differences (bottom line).

3.4.2. Shape-based classification

The classification algorithm with the highest sex classification accuracy and its corresponding accuracy were identified. Additionally, the most significant shape variation—represented by the principal component (PC)—for sex classification was determined using the ANOVA Feature Ranking Algorithm (Table 2). Figure 9 visually illustrates these shape variations.

When assessing classification accuracy without considering age, an overall accuracy of 81% was achieved. PC1, which accounts for the greatest variance in the data, emerged as the most significant shape variation for distinguishing between sexes. The "All" section of Figure 9 showed that PC1 primarily represents variation in the dorsal-ventral width of the symphyseal surface.

An analysis of results by age group revealed a notable trend: sex classification accuracy increased with age, peaking at 94.4% in individuals in their 50s. After the 50s, accuracy slightly declined but remained stable. Across all age groups except for the 20s and 30s, PC1 consistently represented the most significant shape variation for distinguishing between sexes.

As illustrated in Figure 9, the significant shape variations in each age group, except for the 20s and 30s, primarily reflected differences in dorsal-ventral width, consistent with the findings for the overall population. In contrast, the 20s and 30s exhibited more complex shape variations involving the overall outline and surface details. In the 20s, the most prominent variation occurred in the surface volume at the center, along with the ventral tilting of the superior angle. This tilting also produced a notch on the ventral margin. In the 30s, the pattern of shape variation resembled that of the 20s, but the magnitude of differences in surface volume and the tilting of the superior angle was less pronounced.

Table 2. Sex estimation training performance.

Age groups	Best performing algorithm	Accuracy (%)	Best PC number*
All	Logistic Regression Kernel	81.0	1
20s	Kernal Naïve Bayes	75.0	3
30s	Logistic Regression Kernel	80.6	2
40s	Dense Tree	86.1	1
50s	Efficient Linear SVM	94.4	1
60s	Logistic Regression Kernel	83.3	1
70s	Bagged Tree	83.3	1
80s	Efficient Logistic Regression	83.3	1

* The most significant shape variation (PC) for sex classification. Ranked based on ANOVA Feature Ranking Algorithm.

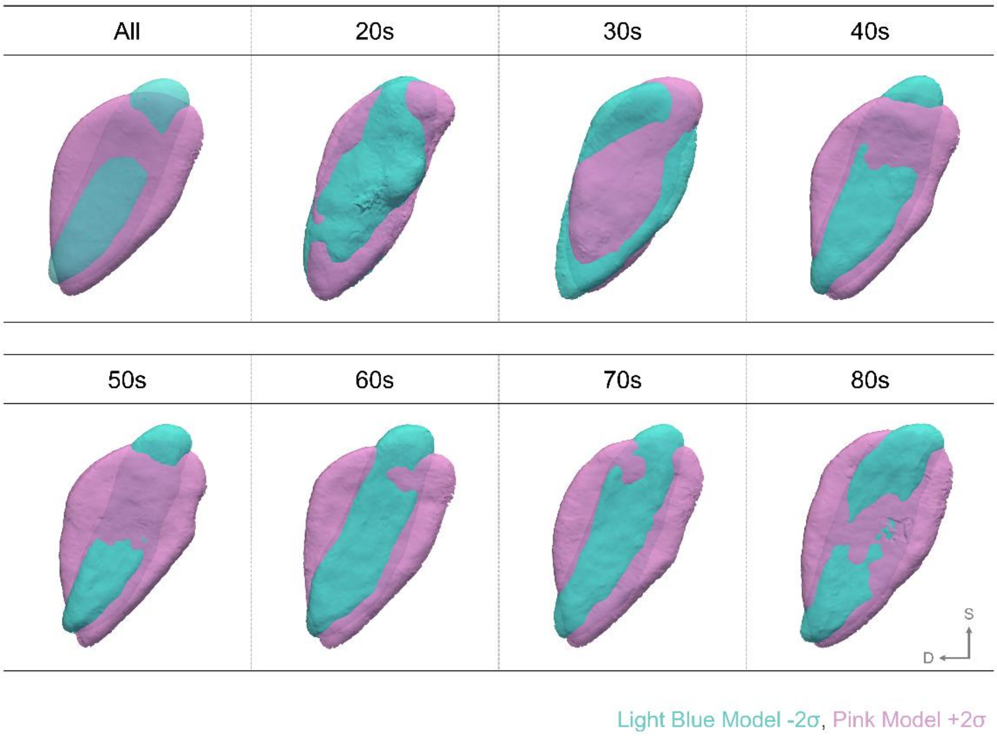

Figure 9. Significant shape variation for sex classification in each age group.

A model with a weight of -2 standard deviations (light blue) and one with a weight of +2 standard deviations (pink) are superimposed. The areas of overlap between the two models are shown in colors other than light blue or pink.

3.5. Aging Morphology

3.5.1. Model comparison

Age-related morphological changes in the mean pubic symphysis models for each age group were visualized (Figure 10), and their statistical significance was assessed (Figure 11). For analysis, the sample data were categorized into three age groups: young adults (YA), middle-aged adults (MA), and older adults (OA).

In males and females, the most pronounced morphological changes occurred in the YA group, particularly during the transition from the 20s to the 30s. In subsequent age transitions, the magnitude of change gradually decreased, with slight increases observed in the MA group—specifically from the 50s to the 60s in males and from the 40s to the 50s in females. While males exhibited a sharp reduction in the rate of morphological change with increasing age, females demonstrated a more gradual decline across all age groups, except beyond the 60s. Additionally, males displayed more statistically significant morphological changes than females, whose changes were less pronounced.

The focal points of morphological changes shifted with age. In the YA group, the changes were primarily concentrated on surface characteristics. In contrast, in the MA and OA groups, the alterations were more prominent in the surface outline for both sexes. Furthermore, when constructing a shape model without separating the sexes, the pattern of morphological change closely resembled that observed in males.

The detailed findings are as follows.

In the YA group, the pubic symphysis, regardless of sex, tended to extend toward both the ventral and dorsal margins. Significant changes were evident near the ventral margin during the transition from the 20s to the 30s. In comparison, prominent alterations appeared near the dorsal margin during the transition from the 30s to the 40s. In males, distinct modifications were observed near the center of the ventral margin between the 20s and 30s. In contrast, females exhibited morphological changes in the same regions; however, these changes were not statistically significant.

In the MA group, both sexes experienced a slight increase in the magnitude of change. In males, statistically significant alterations occurred primarily in the superior half of the surface. At the same time, changes were concentrated along the ventral and dorsal margins in females, though these changes did not reach statistical significance.

Finally, both sexes exhibited minimal morphological changes in the OA group, and statistically significant alterations were largely absent.

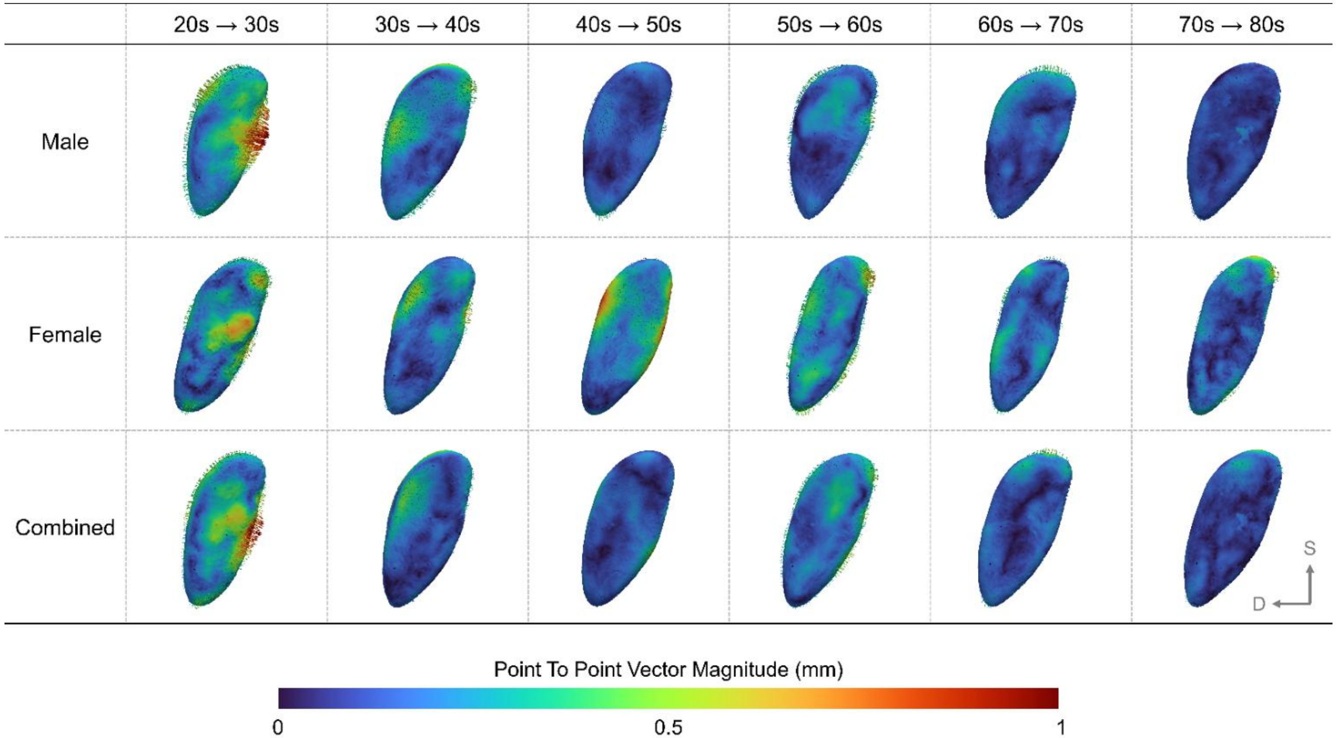

Figure 10. Shape comparison between consecutive age groups.

Three-dimensional visualization of the relative difference in the pubic symphysis between older and younger age groups, with vector arrows indicating the direction and magnitude of changes, doubled in size for clarity.

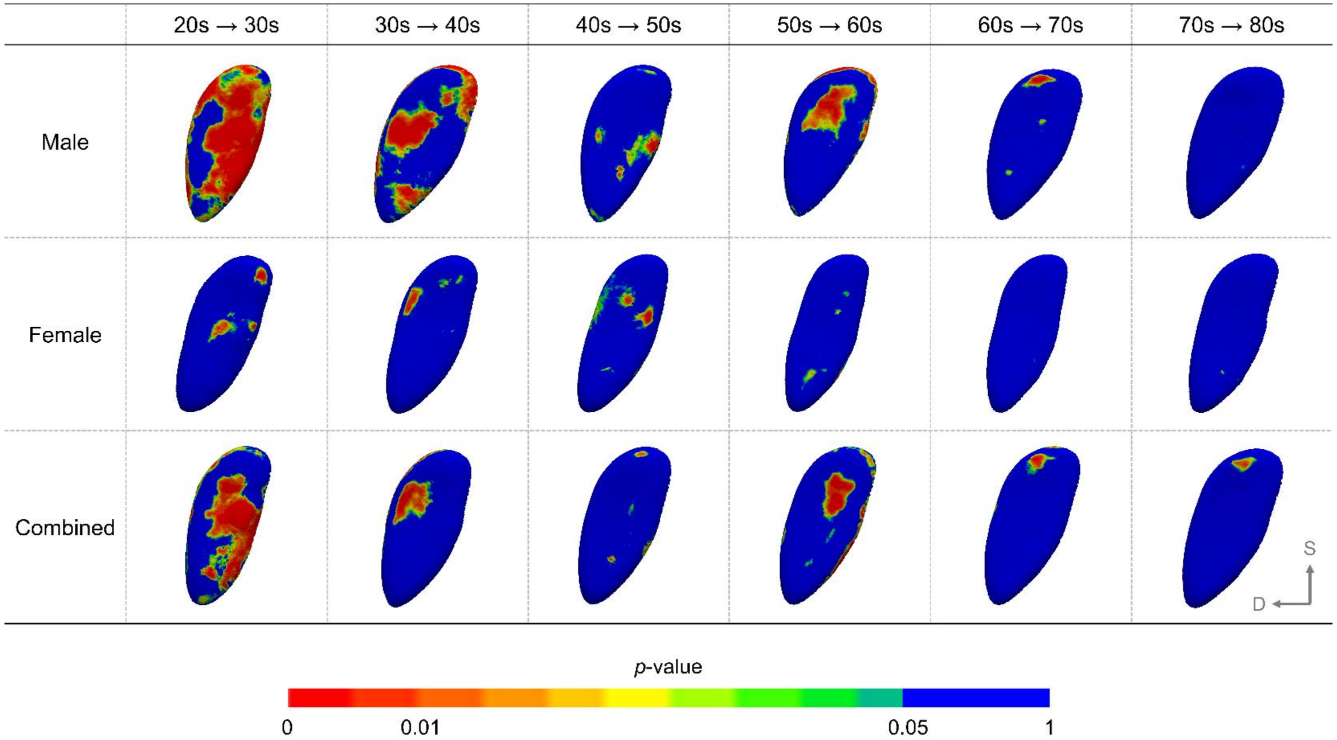

Figure 11. Statistical testing of age-related morphological changes.

Regions with p-values above 0.05 are shown in blue, while those below 0.05 are color-coded by significance level, with the most significant changes marked in red.

3.5.2. Shape-based classification

The classification algorithm with the highest accuracy and corresponding accuracy for each age-sex group was determined. Additionally, the most significant shape variation, represented by the PC, for age classification was identified (Table 3). Figure 12 visually represents these shape variations for each age-sex group.

As shown in Table 3, the transition from the 20s to the 30s produced the highest age classification accuracy for both males and females. Accuracy also slightly increased during specific transitions: from the 50s to the 60s in males, from the 40s to the 50s in females, and from the 70s to the 80s in females. Except for the transitions from the 70s to the 80s in males and from the 50s to the 60s in females, separating the sexes for age classification consistently resulted in higher accuracy than combining both sexes in the analysis.

The analysis also revealed an interesting trend: lower-ranked PCs (i.e., PCs explaining the greatest variance) played a more significant role in distinguishing consecutive age groups when classification accuracy was relatively high. This pattern was particularly evident during the transitions from the 20s to the 30s, the 30s to the 40s, and the 50s to the 60s.

For significant shape variations (Figure 12), surface details consistently appeared in all PCs across every group. However, the observed surface shape variations were challenging to define due to their irregular nature. When males and females were analyzed together, surface details emerged as one of the most significant factors for classifying age groups, except for the most significant PC during the 20s–30s transition. In this case, the PC primarily reflected curvature along the ventral or dorsal margins.

The age-related shape variations by group were as follows.

In addition to sex-based differences in the YA group, the analysis highlighted distinct variations during the transitions from the 20s to the 30s and the 30s to the 40s. During the

20s–30s transition, males primarily exhibited variations in symphyseal surface width, which served as the most critical factor for classification. The second most significant variation was the ventral or dorsal margins curvature. The extent of surface protrusion emerged as the most crucial factor for females, mirroring the secondary factor identified in males. Additionally, irregular surface characteristics emerged as a key distinguishing feature in females. During the 30s–40s transition, males and females displayed similar patterns of significant shape variations. The primary factors were the sharpness of the inferior point and the notch formation along the ventral margin. Additional factors included the length of the pubic symphysis and detailed surface features embedded in the PCs.

Significant PCs consistently captured surface details in both the MA and OA groups. These surface details appeared irregular and resisted standardization into definitive descriptions. However, in the OA group, the most critical PCs captured more complex patterns of surface variation, reflecting the increasing morphological intricacy in this age group.

Table 3. Age estimation training performance.

Age groups	Sex	Best performing algorithm	Accuracy (%)	Best PC number*
20s – 30s	M	Logistic Regression Kernel	83.3	1
	F	Gaussian Naïve Bayes	83.3	4
	All	SVM Kernel	77.8	2
30s – 40s	M	Efficient Logistic Regression	80.6	3
	F	Bagged Tree	72.2	6
	All	Efficient Logistic Regression	70.8	7
40s – 50s	M	Bagged Tree	66.7	6
	F	Bagged Tree	75.0	8
	All	Kernel Naïve Bayes	65.3	52
50s – 60s	M	Logistic Regression Kernel	83.3	4
	F	Fine Tree	61.1	6
	All	Coarse Tree	63.9	4
60s – 70s	M	Binary GLM Logistic Regression	77.8	11
	F	Medium Neural Network	66.7	17
	All	Medium KNN	58.3	11
70s – 80s	M	Binary GLM Logistic Regression	63.9	20
	F	Binary GLM Logistic Regression	77.8	30
	All	Three-dimensional KNN	66.7	11

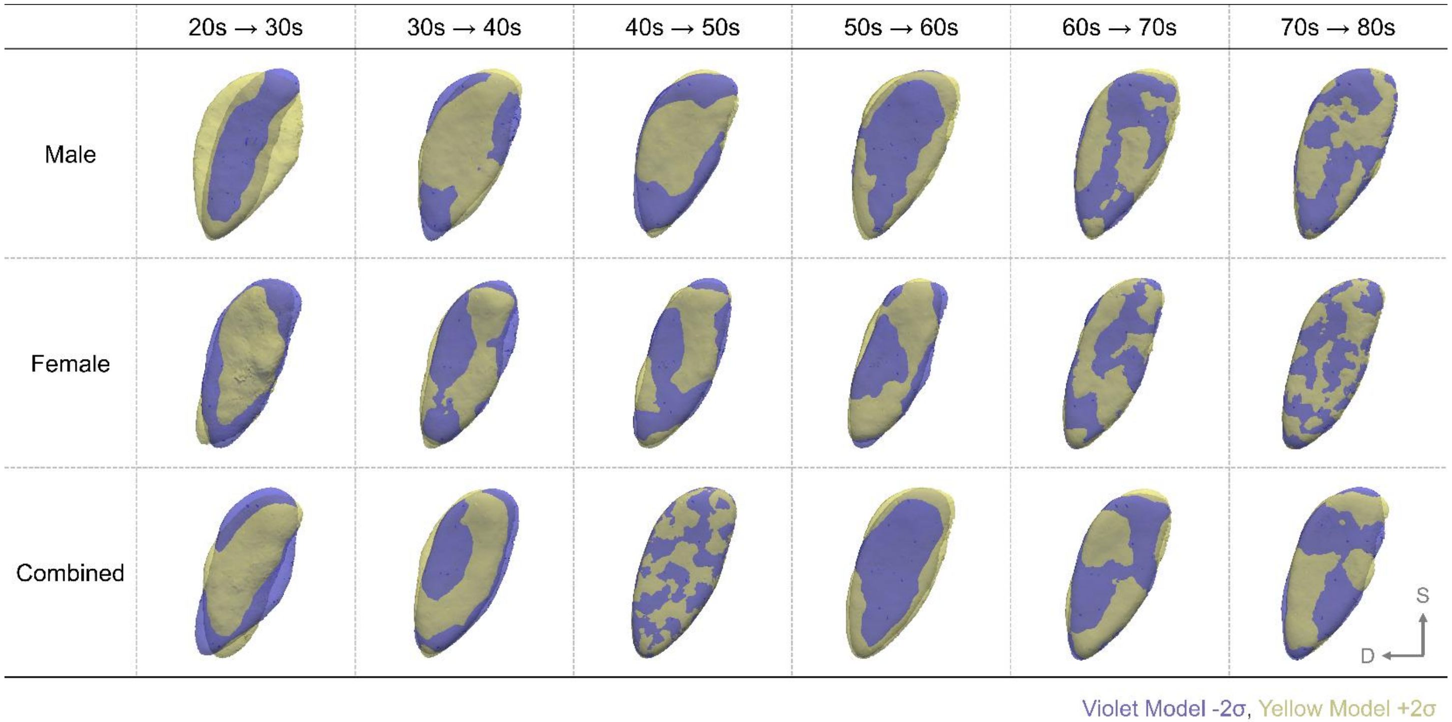

Figure 12. Significant shape variation for classifying two successive age groups.

A model with a weight of -2 standard deviations (violet) and one with a weight of +2 standard deviations (yellow) are superimposed. The two models' overlap areas are shown in colors other than violet or yellow.

4. Discussion

4.1. Principal components

PCA reduces the dimensionality of data by emphasizing axes with the highest variance (68). Higher-ranked PCs are typically regarded as effective in capturing significant patterns within a dataset. As a result, numerous biological anthropology research has focused on these higher-ranked PCs to distinguish variables such as age and sex based on skeletal morphology. However, the primary role of high-ranked PCs is to reflect the dominant shape variations in the dataset, highlighting individual variations instead of directly providing clear indicators for age or sex classification. Conversely, lower-ranked PCs, which are often dismissed as noise during dimensionality reduction, can reveal subtle and localized patterns in the data that are crucial for specific classification tasks (68-71).

In this study, higher-ranked PCs derived from the PCA of 252 pubic symphyses (Figure 4) demonstrated significant associations with sexual dimorphism but not with age group classification. PCs with high explained variance were effective for sex classification (Table 2). However, as shown in Table 3, comparisons among older age groups revealed that shape variations with lower explained variance were more effective in distinguishing between age groups. This finding suggests that, in the pubic symphysis, subtle and localized patterns become increasingly important for age differentiation as individuals age.

In this study, age group differentiation relied on comparisons between consecutive groups, limiting the identification of variations across a broader age range. Expanding the approach to include the entire spectrum from 20 to 80 could establish more reliable indicators for distinguishing young, middle-aged, and older adults. Despite these limitations, the findings address key shortcomings of traditional visual age estimation methods, which often rely on broad and overlapping age categories.

4.2. Sexual dimorphism

4.2.1. Model comparison

When analyzing the morphological differences between males and females without dividing by age groups, this study observed a notable tendency for the dorsal border to shift toward the center of the surface. This finding aligns with a former study by Bravo Morante et al., the primary reference for this study, and Todd, who reported that the dorsal border appears flatter in females (22,44). However, unlike previous studies, this research also identified a flattening trend in the ventral border, albeit to a lesser extent than in the dorsal border.

Furthermore, the superior angle tended to extend upward. While previous studies suggested that a flatter dorsal border contributed to an elongated appearance in females (44), this study demonstrated that the elongated appearance results from a combination of dorsal and ventral border flattening and the superior angle extending superiorly. In addition, although previous studies did not address changes in the inferior point, this study found that the inferior point in females showed a dorsal tilt, adding a novel contribution to the understanding of pubic symphyseal morphology.

Despite these findings, the statistical testing in this study indicated that changes across almost all areas were statistically significant. While this may suggest that all observed morphological changes are genuinely meaningful, the considerable inter-individual morphological variation in the dataset used in this study might have influenced the detection of statistically significant results. Therefore, further validation using datasets with different population groups is necessary to confirm these findings.

Some research has suggested that sexual dimorphism increases significantly after puberty and differs from age to age (22,24). However, previous studies that analyzed the sexual dimorphism of the pubic symphysis did so without distinguishing between age groups or by simply dividing the groups into young, middle-aged, and older adults (44). Therefore, this study investigates sexual dimorphism across different age groups.

From the 30s onward, sexual dimorphism predominantly appears in the outline, consistent with observations when age groups are not separated. As reported in previous studies, the most pronounced sexual dimorphism is observed in the ventral and dorsal borders, particularly in the dorsal-ventral width (22,44). While earlier research primarily noted a sharp increase in sexual dimorphism beginning in the 30s, this study extends these findings by identifying additional, more nuanced aspects of this phenomenon.

Sexual dimorphism indeed becomes evident in the 30s. Prior research has linked a surge in sexual dimorphism in the 30s to pregnancy and childbirth as it changes bone density (44,72-75). In the Korean population, the subject of this study, the average age of first childbirth is 33 years old (76). Therefore, as previously agreed, it is plausible to infer that factors like pregnancy and childbirth contributed to the observed flattening of the ventral border in the 30s. Nevertheless, further physiological and biomechanical validation is required to clarify the mechanisms underlying this pattern. However, contrary to earlier studies that emphasized the flattening of the dorsal border (22,44), this research demonstrates that 30s sexual dimorphism is primarily concentrated on the ventral border. By contrast, significant changes in the dorsal border did not emerge until the 40s.

This study also identifies, for the first time, that sexual dimorphism peaks in the 50s. Bone density typically declines in males and females between the ages of 35 and 45; however, this decline accelerates in females due to menopause, resulting in more pronounced bone density differences in the 40s (77-80). These physiological changes, combined with the sexual dimorphism already present in the 30s, likely led to the peak observed in the 50s.

The results for individuals in their 20s diverge significantly from the findings of previous studies. Previous studies assumed that sexual dimorphism was most evident on the outline (44). However, this study demonstrated that in the 20s, sexual dimorphism is more prominently reflected in surface volume rather than outline. In females, statistically significant differences were found as dorsal tilting of the superior and inferior angles and increased volume in the central ventral region of the symphyseal surface. This finding suggests that in the 20s, sexual dimorphism could not be effectively distinguished by outline alone but instead requires an analysis of surface morphology.

4.2.2. Shape-based classification

Without separating by age groups, the significant shape variation for distinguishing between sexes was the dorsal-ventral width. This finding aligns with previous studies, as discussed in the 4.1.1 section, which noted that females exhibit a more elongated appearance than males (22,44).

Breaking the findings down by age groups, this study identifies PC1 as the most significant principal component for distinguishing between sexes from the 40s to the 80s. These findings align with the overall results without separating them by age, where dorsal-ventral width appears as the primary indicator of sexual dimorphism (22,44). In addition, the previous study described female pubic symphysis as having an "elongated appearance," implying a perceived lengthening (44). However, this study confirms that the pubic symphysis in females is superiorly longer. Moreover, individuals in their 50s show the highest accuracy in sex classification, coinciding with the peak of sexual dimorphism. This result suggests that the pubic symphysis in the 50s allows for a more apparent distinction between sexes compared to other age groups.

The age groups requiring closer attention are those in their 20s and 30s. The lower accuracy in distinguishing age groups in the 20s and 30s compared to older groups, such as those in their 60s and beyond, indicates that sexual dimorphism is relatively less pronounced in younger adults. While previous studies and the findings discussed in Section 4.1.1 noted the emergence of sexual dimorphism in the 30s, the relatively weak degree of dimorphism at this stage indicates that it is still in an early developmental phase (44).

Additionally, unlike other age groups, the significant shape variations in the 20s and 30s do not involve dorsal-ventral width. Figure 9 demonstrated that the shape variations in the 20s and 30s primarily concern whether the surface volume is concentrated along the dorsal and ventral borders or the central region. In the 30s, however, this trend appears less pronounced compared to the 20s. As highlighted in Section 4.1.1, these findings suggest that distinguishing sex in individuals up to their 30s requires focusing on surface details or volume rather than outline.

Another notable feature in the 20s and 30s involves the upper half of the ventral border, mainly whether it appears curved or straight. Combining this observation with the model comparison results (Figure 8) reveals that females tend to have a rounded, curved ventral border. At the same time, males display a straighter upper half, forming an angular shape near the middle. This finding differs significantly from Bravo Morante et al.'s 2021 study, which proposed distinct representative pubic symphyseal morphologies for young adult males and females (44). Furthermore, the observation that males have a straighter ventral border challenges Bravo Morante et al.'s conclusion that males tend to exhibit a more rounded shape (44). However, as this study focused on the Korean population, validation in other populations for broader applicability is required.

4.3. Aging morphology

4.3.1. Model comparison

The observations in the YA group align with previous studies, confirming that younger age groups experience more pronounced morphological changes and are easier to distinguish than other age groups (37,39,41,42). However, the transition from the 20s to the 30s reveals distinct patterns of change between males and females, underscoring the significant influence of sex beyond aging effects.

In males, the marked extension at the center of the ventral margin coincides with the superior margin of the suspensory ligament that supports the base of the penis, where it attaches to the pubic symphysis (81). This extension likely results from the greater tension exerted by the suspensory ligament due to the protrusion of external male genitalia. However, further anatomical studies are necessary to elucidate the correlation between suspensory ligaments and aging, particularly in young adults.

The morphological changes observed during this transition were not statistically significant in females. This result may reflect fluctuating individual differences caused by external factors, such as pregnancy, rather than natural aging processes. South Korean women have their first childbirth at an average age of 33.5 years, with childbirth rates peaking in their 30s (76). Pregnancy and childbirth can alter pelvic floor muscles, leading to changes such as weakening and sagging (82-84). Since these muscles connect to the pubic bone (84), maternity status could plausibly influence the morphology of the pubic symphysis during this specific age range. However, as this study lacked data on the pregnancy and childbirth histories of the subjects, future research should examine age-related changes while accounting for maternity status.

From the 30s to 40s, males and females exhibited similar patterns of morphological changes, but the exact locations of these changes differed. In males, changes occurred near the origins of the rectus abdominis, pyramidalis, and gracilis muscles, while in females, the adductor longus muscle origin showed more pronounced changes (85-87). As suggested in previous studies, variations in muscle usage may influence pubic symphyseal morphology (51). However, specific research focusing on the primary muscles utilized by males and females within this age group still needs to be completed, underscoring the need for further investigation.

In the MA group, males in their 50s and females in their 40s exhibited a sudden surge in the rate of change. This shift may correspond to age-related bone loss, which typically begins in both sexes around 35–40 years of age. Physiological differences likely explain the more significant changes observed in females than males (77,78,80). Females experience accelerated bone loss during their 40s and early 50s due to menopause, whereas males undergo a more gradual loss over their lifetime (77,79,80).

The patterns of change also varied between sexes. In males, the observed changes aligned with established pubic symphyseal aging processes characterized by surface smoothing (37,41). Conversely, females showed a pattern of narrowing pubic symphyseal width, contrasting with findings by Lottering et al., who reported increasing maximum width with aging to maintain mechanical strength (45). However, caution is advised when interpreting these findings because these changes in females were not statistically significant.

The results in the OA group challenge findings by Kotěrová et al., who suggested that age-related differences remain distinguishable even in individuals over 50 years old (42). In this study, statistically significant morphological changes were difficult to identify in both sexes after 60 years of age. The changes observed in this age group likely reflect irregular individual variations rather than consistent aging patterns across the population (40,41,88,89).

Morphological changes in older females were particularly notable. While these changes did not achieve statistical significance, their moderate presence suggests greater individual variability among aging females compared to males. This finding contradicts earlier studies suggesting females exhibit less individual variability in pubic symphyseal morphology than males (37). As discussed in the YA and MA groups, females are more likely to experience physiological events such as childbirth and menopause, which affect pubic symphyseal morphology (23,82). Furthermore, pelvic floor muscles connected to the pubic symphysis undergo more age-related changes in females, including sagging, which increases with age regardless of pregnancy and childbirth history (90,91). These findings and hormonal and muscle-aging patterns suggest that females may exhibit more significant morphological variability with advancing age.

4.3.2. Shape-based classification

In the YA group, it was necessary to analyze transitions from the 20s to the 30s and from the 30s to the 40s separately due to differences in significant shape variations. The ventral-dorsal width was the most critical shape variation distinguishing males in their 20s from those in their 30s. This finding aligns with previous research, which reported an increase in the superior-inferior and ventral-dorsal dimensions of the symphyseal surface with age (45). However, apart from this transition, width did not emerge as a decisive factor in other groups. This suggests that ventral-dorsal width alone may not be sufficient for general age classification. However, it is more relevant for distinguishing adolescents and young adults in their 20s from other age groups among male specimens.

Additionally, the second most crucial factor distinguishing males in their 20s and 30s was the curvature of the margin. This observation supports findings that describe the symphyseal surface transitioning to a more rounded shape after age 30 (40). For females, this curvature was identified as the most significant shape variation during the 20s–30s transition but carried less significance, likely reflecting greater individual variability within this age group.

During the 30s–40s transition, both males and females prioritized the minor notch-like feature located on the upper one-third of the ventral border as a distinguishing factor. This observation corresponds to Phase IV of the Suchey and Brooks method, which described a hiatus on the upper ventral rim. It also aligns with findings from subsequent geometric morphometric studies (25,35,44). However, previous research either suggested a broad age range for the appearance of the notch or associated it with older adults without specifying a particular age group. While this study did not exclusively determine age groups for notch formation, the findings, in conjunction with previous research, suggest that the notch is absent until the 30s and emerges during the 40s. The underlying cause of this phenomenon remains unexplored. Recent studies on the morphology of the four ligaments surrounding the pubic symphysis revealed that the notch formation area overlaps with the superior and anterior pubic ligaments (92). This overlap may contribute to notch formation, but future biomechanical studies are needed to validate this hypothesis.

In the MA and OA groups, significant shape variations distinguishing age groups primarily involved complex surface textures, which posed challenges for standardized descriptions. This finding explains why computational methods capable of analyzing subtle surface details through algorithms can improve age estimation accuracy. However, previous studies that calculated morphological changes using bending energy scores often overestimated these scores due to surface irregularities, resulting in underestimation of the age of older individuals (41). The patterns of surface shape variation identified in this study could help address such errors in future research.

Moreover, more complex surface shape variations were observed in females than males. Previous studies predominantly focused on males or used mixed-sex samples (40-42). While mixed-sex analyses may be helpful when sex cannot be determined, when sex is identifiable, sex-specific estimation methods should be employed. This study highlights the importance of developing separate age estimation approaches for each sex to improve accuracy.

5. Conclusion

This study addresses critical limitations in previous research on pubic symphysis morphology within biological anthropology. Traditional visual analyses of the pubic symphysis, such as those by Todd and Suchey-Brooks, emphasize sex-specific differences. Still, previous studies have lacked detailed three-dimensional analyses of sexual dimorphism. Additionally, while computational methods for age estimation achieved high accuracy, they obscured the specific morphological features that drive classification, creating a "black box."

By utilizing SSM, this study overcame these limitations and provided a detailed analysis of sexual dimorphism and age-related morphological changes in the pubic symphysis. Though SSM is widely used in various fields, its application in biological and forensic anthropology remains rare. This study aimed to reveal critical morphological patterns and provide a transparent framework for interpreting skeletal morphology by employing SSM.

The findings of this study are summarized as follows:

- Three-dimensional visualization of sexually dimorphic morphologies between males and females.
- Identification of crucial shape variations for distinguishing between sexes.
- Three-dimensional visualization of age-related changes in each age-sex group.
- Determination of crucial shape variations for differentiating consecutive age groups

These results deepen our understanding of pubic symphyseal morphology and highlight the potential of SSM as a tool in anthropological research.

However, this study has several limitations that require further investigation. The exclusive focus on the Korean population necessitates the inclusion of diverse population groups to generalize the findings. For female subjects, analyzing medical history—such as pregnancy, childbirth, and menopause—can enhance the accuracy of detecting statistically significant morphological changes in female subjects. Additionally, the use of PCA for only two consecutive age groups makes it challenging to apply the findings of this study when pubic symphyses from a broader range of age groups are intermixed. Future research should conduct PCA on multiple age groups to provide a more comprehensive understanding of age-related morphological patterns. Finally, while this study hypothesizes that the muscles' biomechanical effects contribute to morphological differences and changes in the pubic symphysis, these hypotheses require validation. Interdisciplinary research integrating biomechanical methods, such as finite element analysis, can confirm these effects and refine understanding of these influences.

Despite these limitations, this study highlights the complexity of sexual dimorphism and age-related changes in the pubic symphysis. By employing advanced methodologies and offering valuable insights, this research not only advances the understanding of pubic symphysis morphology but also lays a strong foundation for future studies in biological anthropology.

REFERENCES

1. Haas J, Buikstra JE, Ubelaker DH, Aftandilian D, History FMoN, Survey AA. Standards for Data Collection from Human Skeletal Remains: Proceedings of a Seminar at the Field Museum of Natural History, Organized by Jonathan Haas: Arkansas Archeological Survey; 1994.

2. White TD, Black MT, Folkens PA. Chapter 18 - Assessment of Age, Sex, Stature, Ancestry, and Identity of the Individual. In: White TD, Black MT, Folkens PA, editors. Human Osteology (Third Edition). San Diego: Academic Press; 2012. p. 379-427.

3. Lynnerup N. Forensic anthropology and human identification. Scandinavian Journal of Forensic Science. 2013;19(1):16-38.

4. Tague RG. Sexual dimorphism in the human bony pelvis, with a consideration of the Neandertal pelvis from Kebara cave, Israel. American Journal of Physical Anthropology. 1992;88(1):1-21.

5. Arsuaga JL, Carretero JM. Multivariate analysis of the sexual dimorphism of the hip bone in a modern human population and in early hominids. American Journal of Physical Anthropology. 1994;93(2):241-57.

6. Walrath DE, Glantz MM. Sexual dimorphism in the pelvic midplane and its relationship to Neandertal reproductive patterns. American Journal of Physical Anthropology. 1996;100(1):89-100.

7. Kurki HK. Pelvic dimorphism in relation to body size and body size dimorphism in humans. Journal of Human Evolution. 2011;61(6):631-43.

8. Fischer B, Mitteroecker P. Covariation between human pelvis shape, stature, and head size alleviates the obstetric dilemma. Proceedings of the National Academy of Sciences. 2015;112(18):5655-60.

9. Fischer B, Mitteroecker P. Allometry and Sexual Dimorphism in the Human Pelvis. The Anatomical Record. 2017;300(4):698-705.

10. Phenice TW. A newly developed visual method of sexing the os pubis. American Journal of Physical Anthropology. 1969;30(2):297-301.

11. Acsádi G, Nemeskéri J. History of Human Life Span and Mortality: Akadémiai Kiadó; 1970.

12. Loth SR, Henneberg M. Mandibular ramus flexure: a new morphologic indicator of sexual dimorphism in the human skeleton. Am J Phys Anthropol. 1996;99(3):473-85.

13. Graw M, Czarnetzki A, Haffner H-T. The form of the supraorbital margin as a criterion in identification of sex from the skull: Investigations based on modern human skulls. American Journal of Physical Anthropology. 1999;108(1):91-6.

14. Kimmerle EH, Prince DA, Berg GE. Inter-Observer Variation in Methodologies Involving the Pubic Symphysis, Sternal Ribs, and Teeth. Journal of Forensic Sciences. 2008;53(3):594-600.

15. Saunders SR, Fitzgerald C, Rogers T, Dudar C, McKillop H. A Test of Several Methods of Skeletal Age Estimation using a Documented Archaeological Sample. Canadian Society of Forensic Science Journal. 1992;25(2):97-118.

16. Hens SM, Rastelli E, Belcastro G. Age Estimation from the Human Os Coxa: A Test on a Documented Italian Collection. Journal of Forensic Sciences. 2008;53(5):1040-3.

17. Fanton L, Gustin M-P, Paultre U, Schrag B, Malicier D. Critical Study of Observation of the Sternal End of the Right 4th Rib. Journal of Forensic Sciences. 2010;55(2):467-72.

18. Miles AEW. Dentition in the Estimation of Age. Journal of Dental Research. 1963;42(1):255-63.

19. Lovejoy CO. Dental wear in the Libben population: Its functional pattern and role in the determination of adult skeletal age at death. American Journal of Physical Anthropology. 1985;68(1):47-56.

20. Meindl RS, Lovejoy CO. Ectocranial suture closure: a revised method for the determination of skeletal age at death based on the lateral-anterior sutures. Am J Phys Anthropol. 1985;68(1):57-66.

21. Key CA, Aiello LC, Molleson T. Cranial suture closure and its implications for age estimation. International Journal of Osteoarchaeology. 1994;4(3):193-207.

22. Todd TW. Age changes in the pubic bone. I. The male white pubis. American Journal of Physical Anthropology. 1920;3(3):285-334.

23. Gilbert BM, McKern TW. A method for aging the female Os pubis. American Journal of Physical Anthropology. 1973;38(1):31-8.

24. Meindl RS, Lovejoy CO, Mensforth RP, Walker RA. A revised method of age determination using the os pubis, with a review and tests of accuracy of other current methods of pubic symphyseal aging. American Journal of Physical Anthropology. 1985;68(1):29-45.

25. Brooks S, Suchey JM. Skeletal age determination based on the os pubis: A comparison of the Acsádi-Nemeskéri and Suchey-Brooks methods. Human Evolution. 1990;5(3):227-38.

26. Işcan MY, Loth SR, Wright RK. Metamorphosis at the sternal rib end: a new method to estimate age at death in white males. Am J Phys Anthropol. 1984;65(2):147-56.

27. Singh J, Chavali KH. Age estimation from clavicular epiphyseal union sequencing in a Northwest Indian population of the Chandigarh region. J Forensic Leg Med. 2011;18(2):82-7.

28. Lovejoy CO, Meindl RS, Pryzbeck TR, Mensforth RP. Chronological metamorphosis

of the auricular surface of the ilium: a new method for the determination of adult skeletal age at death. Am J Phys Anthropol. 1985;68(1):15-28.

29. Garvin HM, Passalacqua NV. Current Practices by Forensic Anthropologists in Adult Skeletal Age Estimation*. Journal of Forensic Sciences. 2012;57(2):427-33.

30. McKern TW, Stewart TD. Skeletal Age Changes in Young American Males, Analysed from the Standpoint of Age Identification. Technical Report EP-45. 1957.

31. Katz D, Suchey JM. Age determination of the male Os pubis. American Journal of Physical Anthropology. 1986;69(4):427-35.

32. Hughes C, Yim A-D, Juarez C. Considerations for age estimation accuracy: Method-derived outcomes and practitioner interpretations. Journal of Forensic Sciences.n/a(n/a).

33. Kimmerle EH, Prince DA, Berg GE. Inter-Observer Variation in Methodologies Involving the Pubic Symphysis, Sternal Ribs, and Teeth*. Journal of Forensic Sciences. 2008;53(3):594-600.

34. Berg GE. Pubic Bone Age Estimation in Adult Women*. Journal of Forensic Sciences. 2008;53(3):569-77.

35. Hartnett KM. Analysis of Age-at-Death Estimation Using Data from a New, Modern Autopsy Sample—Part I: Pubic Bone*,†. Journal of Forensic Sciences. 2010;55(5):1145-51.

36. Biwasaka H, Sato K, Aoki Y, Kato H, Maeno Y, Tanijiri T, et al. Three dimensional surface analyses of pubic symphyseal faces of contemporary Japanese reconstructed with 3D digitized scanner. Legal Medicine. 2013;15(5):264-8.

37. Villa C, Buckberry J, Cattaneo C, Frohlich B, Lynnerup N. Quantitative Analysis of the Morphological Changes of the Pubic Symphyseal Face and the Auricular Surface and Implications for Age at Death Estimation. Journal of Forensic Sciences.

2015;60(3):556-65.

38. Slice DE, Algee-Hewitt BFB. Modeling Bone Surface Morphology: A Fully Quantitative Method for Age-at-Death Estimation Using the Pubic Symphysis. Journal of Forensic Sciences. 2015;60(4):835-43.

39. Stoyanova D, Algee-Hewitt BFB, Slice DE. An enhanced computational method for age-at-death estimation based on the pubic symphysis using 3D laser scans and thin plate splines. American Journal of Physical Anthropology. 2015;158(3):431-40.

40. Stoyanova DK, Algee-Hewitt BFB, Kim J, Slice DE. A Computational Framework for Age-at-Death Estimation from the Skeleton: Surface and Outline Analysis of 3D Laser Scans of the Adult Pubic Symphysis. Journal of Forensic Sciences. 2017;62(6):1434-44.

41. Bravo Morante G, Bookstein FL, Fischer B, Schaefer K, Alemán Aguilera I, Botella López MC. Correlation of the human pubic symphysis surface with age-at-death: a novel quantitative method based on a bandpass filter. International Journal of Legal Medicine. 2021;135(5):1935-44.

42. Kotěrová A, Štepanovský M, Buk Z, Brůžek J, Techataweewan N, Velemínská J. The computational age-at-death estimation from 3D surface models of the adult pubic symphysis using data mining methods. Scientific Reports. 2022;12(1):10324.

43. Castillo A, Galtés I, Crespo S, Jordana X. Technical note: preliminary insight into a new method for age-at-death estimation from the pubic symphysis. International Journal of Legal Medicine. 2021;135(3):929-37.

44. Bravo Morante G, Fischer B, Botella López MC, Bastir M. The outline of the pubic symphyseal surface is sexually dimorphic and changes with age in humans. J Anthropol Sci. 2021;99:83-95.

45. Lottering N, Reynolds MS, MacGregor DM, Meredith M, Gregory LS. Morphometric

modelling of ageing in the human pubic symphysis: Sexual dimorphism in an Australian population. Forensic Science International. 2014;236:195.e1-.e11.

46. Trinkaus E. Bilateral asymmetry of human skeletal non-metric traits. American Journal of Physical Anthropology. 1978;49(3):315-8.

47. Goparaju A, Iyer K, Bône A, Hu N, Henninger HB, Anderson AE, et al. Benchmarking off-the-shelf statistical shape modeling tools in clinical applications. Medical Image Analysis. 2022;76:102271.

48. MARDIA KV, DRYDEN IL. The statistical analysis of shape data. Biometrika. 1989;76(2):271-81.

49. Thompson DAW, Bonner JT. On Growth and Form: Cambridge University Press; 1992.

50. Heimann T, Meinzer H-P. Statistical shape models for 3D medical image segmentation: A review. Medical Image Analysis. 2009;13(4):543-63.

51. Audenaert EA, Pattyn C, Steenackers G, De Roeck J, Vandermeulen D, Claes P. Statistical Shape Modeling of Skeletal Anatomy for Sex Discrimination: Their Training Size, Sexual Dimorphism, and Asymmetry. Frontiers in Bioengineering and Biotechnology. 2019;7.

52. Zadpoor AA, Weinans H. Patient-specific bone modeling and analysis: The role of integration and automation in clinical adoption. Journal of Biomechanics. 2015;48(5):750-60.

53. Fallon Verbruggen F, Killen BA, Burssens A, Boey H, Vander Sloten J, Jonkers I. Unique shape variations of hind and midfoot bones in flatfoot subjects—A statistical shape modeling approach. Clinical Anatomy. 2023;36(6):848-57.

54. Patil A, Kulkarni K, Xie S, Bull AMJ, Jones GG. The accuracy of statistical shape models in predicting bone shape: A systematic review. The International Journal of

Medical Robotics and Computer Assisted Surgery. 2023;19(3):e2503.

55. Lamecker H, Seebass M, Hege H-C, Deuflhard P. Medical Imaging: Image Processing - A 3D statistical shape model of the pelvic bone for segmentation: SPIE; 2004 2004/05/12. 1341-51 p.

56. Ben Younes L, Nakajima Y, Saito T. Fully automatic segmentation of the Femur from 3D-CT images using primitive shape recognition and statistical shape models. International Journal of Computer Assisted Radiology and Surgery. 2014;9(2):189-96.

57. Chan EF, Farnsworth CL, Koziol JA, Hosalkar HS, Sah RL. Statistical shape modeling of proximal femoral shape deformities in Legg–Calvé–Perthes disease and slipped capital femoral epiphysis. Osteoarthritis and Cartilage. 2013;21(3):443-9.

58. Meynen A, Vles G, Zadpoor AA, Mulier M, Scheys L. The morphological variation of acetabular defects in revision total hip arthroplasty—A statistical shape modeling approach. Journal of Orthopaedic Research. 2021;39(11):2419-27.

59. Fliss B, Luethi M, Fuernstahl P, Christensen AM, Sibold K, Thali M, et al. CT-based sex estimation on human femora using statistical shape modeling. American Journal of Physical Anthropology. 2019;169(2):279-86.

60. Shin SM, Kim Y-I, Choi Y-S, Yamaguchi T, Maki K, Cho B-H, et al. The skeletal maturation status estimated by statistical shape analysis: axial images of Japanese cervical vertebra. Dentomaxillofacial Radiology. 2014;44(3).

61. Klop C, Becking AG, Klop C, Koolstra JH, Lobé NHJ, Maal TJJ, et al. A three-dimensional statistical shape model of the growing mandible. Scientific Reports. 2021;11(1):18843.

62. Ebert LC, Rahbani D, Lüthi M, Thali MJ, Christensen AM, Fliss B. Reconstruction of full femora from partial bone fragments for anthropological analyses using statistical shape modeling. Forensic Science International. 2022;332:111196.

63. Cates J, Elhabian S, Whitaker R. Chapter 10 - ShapeWorks: Particle-Based Shape Correspondence and Visualization Software. In: Zheng G, Li S, Székely G, editors. Statistical Shape and Deformation Analysis: Academic Press; 2017. p. 257-98.

64. Ubelaker DH. Human Skeletal Remains: Excavation, Analysis, Interpretation: Taraxacum; 1999.

65. Zelditch ML, Swiderski DL, Sheets HD, Fink WL. 3 - Simple size and shape variables: Bookstein shape coordinates. In: Zelditch ML, Swiderski DL, Sheets HD, Fink WL, editors. Geometric Morphometrics for Biologists. San Diego: Academic Press; 2004. p. 51-72.

66. Elhaik E. Principal Component Analyses (PCA)-based findings in population genetic studies are highly biased and must be reevaluated. Scientific Reports. 2022;12(1):14683.

67. Davies RH, Twining CJ, Cootes TF, Waterton JC, Taylor CJ, editors. 3D Statistical Shape Models Using Direct Optimisation of Description Length. Computer Vision — ECCV 2002; 2002 2002//; Berlin, Heidelberg: Springer Berlin Heidelberg.

68. Jolliffe I. Principal Component Analysis. In: Lovric M, editor. International Encyclopedia of Statistical Science. Berlin, Heidelberg: Springer Berlin Heidelberg; 2011. p. 1094-6.

69. Hawkins DM, Fatti LP. Exploring Multivariate Data Using the Minor Principal Components. Journal of the Royal Statistical Society Series D: The Statistician. 2018;33(4):325-38.

70. Fariha A, Tiwari A, Radhakrishna A, Gulwani S, Meliou A. Conformance Constraint Discovery: Measuring Trust in Data-Driven Systems. Proceedings of the 2021 International Conference on Management of Data; Virtual Event, China: Association for Computing Machinery; 2021. p. 499–512.

71. Zheng J, Rakovski C. On the Application of Principal Component Analysis to Classification Problems. Data Science Journal. 2021.

72. Gur A, Nas K, Cevik R, Sarac AJ, Ataoglu S, Karakoc M. Influence of number of pregnancies on bone mineral density in postmenopausal women of different age groups. J Bone Miner Metab. 2003;21(4):234-41.

73. Huseynov A, Zollikofer CPE, Coudyzer W, Gascho D, Kellenberger C, Hinzpeter R, et al. Developmental evidence for obstetric adaptation of the human female pelvis. Proceedings of the National Academy of Sciences. 2016;113(19):5227-32.

74. Verbruggen SW, Nowlan NC. Ontogeny of the Human Pelvis. The Anatomical Record. 2017;300(4):643-52.

75. Auerbach BM, King KA, Campbell RM, Campbell ML, Sylvester AD. Variation in obstetric dimensions of the human bony pelvis in relation to age-at-death and latitude. American Journal of Physical Anthropology. 2018;167(3):628-43.

76. Kim J, Nam JY, Park E-C. Advanced maternal age and severe maternal morbidity in South Korea: a population-based cohort study. Scientific Reports. 2022;12(1):21358.

77. Clarke BL, Khosla S. Physiology of bone loss. Radiologic clinics of North America. 2010;48 3:483-95.

78. Curtis E, Litwic A, Cooper C, Dennison E. Determinants of Muscle and Bone Aging. Journal of Cellular Physiology. 2015;230(11):2618-25.

79. Warming L, Hassager C, Christiansen C. Changes in Bone Mineral Density with Age in Men and Women: A Longitudinal Study. Osteoporosis International. 2002;13(2):105-12.

80. Baxter-Jones AD, Faulkner RA, Forwood MR, Mirwald RL, Bailey DA. Bone mineral accrual from 8 to 30 years of age: An estimation of peak bone mass. Journal of Bone and Mineral Research. 2011;26(8):1729-39.

81. Hoznek A, Rahmouni A, Abbou C, Delmas V, Colombel M. The suspensory ligament of the penis: an anatomic and radiologic description. Surgical and Radiologic Anatomy. 1999;20(6):413-7.

82. Putschar WGJ. The structure of the human symphysis pubis with special consideration of parturition and its sequelae. American Journal of Physical Anthropology. 1976;45(3):589-94.

83. Alperin M. Chapter Ten - Impact of Pregnancy and Delivery on Pelvic Floor Biomechanics. In: Hoyte L, Damaser M, editors. Biomechanics of the Female Pelvic Floor: Academic Press; 2016. p. 229-38.

84. Stansfield E, Mitteroecker P, Umek W, Fischer B. The variation in shape and thickness of the pelvic floor musculature in males and females: a geometric-morphometric analysis. International Urogynecology Journal. 2023;34(2):453-61.

85. Gamble JG, Simmons SC, Freedman M. The symphysis pubis. Anatomic and pathologic considerations. Clin Orthop Relat Res. 1986(203):261-72.

86. Robertson BA, Barker PJ, Fahrer M, Schache AG. The Anatomy of the Pubic Region Revisited. Sports Medicine. 2009;39(3):225-34.

87. Schilders E, Bharam S, Golan E, Dimitrakopoulou A, Mitchell A, Spaepen M, et al. The pyramidalis–anterior pubic ligament–adductor longus complex (PLAC) and its role with adductor injuries: a new anatomical concept. Knee Surgery, Sports Traumatology, Arthroscopy. 2017;25(12):3969-77.

88. Dudzik B, Langley NR. Estimating age from the pubic symphysis: A new component-based system. Forensic Science International. 2015;257:98-105.

89. Miranker M. A Comparison of Different Age Estimation Methods of the Adult Pelvis. Journal of Forensic Sciences. 2016;61(5):1173-9.

90. Kotarinos RK. Chapter Three - Musculoskeletal Pelvic Anatomy. In: Hoyte L,

Damaser M, editors. Biomechanics of the Female Pelvic Floor: Academic Press; 2016. p. 53-87.

91. Swenson CW, Masteling M, DeLancey JO, Nandikanti L, Schmidt P, Chen L. Aging effects on pelvic floor support: a pilot study comparing young versus older nulliparous women. International Urogynecology Journal. 2020;31(3):535-43.

92. Pieroh P, Li Z-L, Kawata S, Ogawa Y, Josten C, Steinke H, et al. The topography and morphometrics of the pubic ligaments. Annals of Anatomy - Anatomischer Anzeiger. 2021;236:151698.

ABSTRACT IN KOREAN

삼차원 통계적 형태 모델링을 활용한 두덩결합면의 형태적 변동성 분석

두덩결합면은 법의인류학을 비롯한 생물인류학 분야에서 신원미상자의 사망 당시 연령을 추정하는 데 중요한 역할을 한다. 최근 육안 기반의 연령 추정이 가지는 주관성을 개선하고자 다양한 컴퓨터 기반 분석 방법이 개발되었다. 하지만, 이 방법들은 연령 추정에 중요한 형태적 특징을 명확히 밝히지 못하는 "블랙박스" 문제를 포함한 한계를 가진다. 또한, 두덩결합면의 성적 이형성은 잘 알려져 있으나, 관련 연구는 부족하며 표면 변화를 간과하고 윤곽 분석에 주로 의존하고 있다.

이러한 한계를 해결하기 위해 본 연구는 삼차원 통계적 형태 모델링(statistical shape modeling, SSM)을 활용하였다. SSM 은 평균 모델을 생성하고, 미세한 형태 변화를 포착함으로써 한 형태 집단 내의 복잡한 형태 변이를 분석하는데 용이하다. 본 연구에서는 SSM 을 활용하여 두덩결합면의 성적 이형성과 연령에 따른 형태 변화를 분석하였다. 대한민국 국립과학수사연구원에서 제공한 252 명의 사후 컴퓨터 단층촬영 데이터를 활용하였으며, 데이터는 삼차원 파일 형태로 분석하였다. 전처리 된 데이터는 강체 정렬(rigid alignment) 및 통계적 형태 모델 구축을 거쳤고, 평균 모델 간의 비교, 분석을 위해 주성분 분석(principal component analysis)을 수행하였다. 이후 MATLAB 을 활용해 형태 기반 분류 분석을 시행하였다.

성적 이형성은 등-배 폭에서 가장 두드러지게 나타났으며, 30 대에 나타나기 시작하여 50 대에 정점에 도달하였다. 반면, 20 대에서는 윤곽보다 표면 형태에서 더 뚜렷한 성적이형성을 확인할 수 있었다. 연령과 관련된 변화는 젊은 연령층에서 가장 두드러졌으며, 남성은 배 쪽 모서리의 확장이 관찰되는 반면, 여성은 임신과 관련된 것으로 추정되는 형태적 변화가 나타났다. 고령층에서는 형태 변화가 두드러지지

않았으며, 특히 폐경과 골반 근육 노화로 인해 여성 개체 간 형태 차이가 더 크게 나타난 것으로 보인다.

본 연구는 이전까지 법의인류학 분야에서 잘 활용되지 않았던 SSM 을 뼈대 형태 분석에 적용함으로써 두덩결합면의 복잡한 형태적 특성을 규명하는데 기여하였다. 본 연구의 결과는 법의인류학과 생물인류학 분야에서 개인 식별 방법을 발전시키는 중요한 기초 자료로 활용될 것으로 기대된다.

핵심되는 말 : 두덩결합면, 삼차원 통계적 형태 모델링, 성적 이형성, 연령 추정, 개인식별, 법의인류학